STUDY OF ENERGY DEPENDENCE AND ISOTOPIC EFFECT OF TOTAL CROSS SECTIONS FOR FISSION OF Pb, Tl AND Au NUCLEI INDUCED BY PROTONS WITH ENERGIES UP TO 1 GeV

Yu.A. Chestnov, Yu.A. Gavrikov, O.Ya. Fedorov, A.A. Kotov, V.V. Poliakov, A.I. Shchetkovskiy, M.G. Tverskoy, L.A. Vaishnene, V.G. Vovchenko

The need for information concerning fission induced in nuclei by intermediate energy projectiles is obvious. The interest in this process emerges from both fundamental and applied problems of nuclear physics. In spite of extensive experimental efforts, nuclear fission remains insufficiently understood in many aspects. Measurements of the energy dependence of the total cross sections for fission of nuclei by intermediate energy protons will add to our understanding of the fission process in terms of nuclear properties of highly excited nuclei, such as temperature dependence of the level density and fission barriers of excited nuclei. For physics applications, the nuclear data are required for new energy production concepts with the accelerator driven systems (ADS), for nuclear waste transmutation technologies, for accelerator and spacecraft radiation shields. All the above mentioned problems require fission cross section data of high accuracy and reliability. Unfortunately, the majority of experimental fission cross sections, obtained in various experiments with different methods of registration, are dispersed in the range which exceeds the declared accuracy of measurements, not allowing to derive a reliable energy dependence of the fission cross section on the proton energy. High accuracy of fission cross section measurements may be achieved only by modern electronics methods of registration of both fission fragments in coincidence together with high precision monitoring of the proton flux on the studied target. In the present experiment, a method based on the use of gas parallel plate avalanche counters (PPAC) for registration of complementary fission fragments in coincidence and a telescope of scintillation counters for direct counting of incident protons on the target has been applied. This method allowed us to measure the absolute cross sections for proton induced fission of ^{206}Pb, ^{207}Pb, ^{208}Pb, ^{203}Tl and ^{197}Au in the energy range from 200 to 1000 MeV with a step of 100 MeV.

The experiment was performed at the 1 GeV PNPI synchrocyclotron. Since the external proton beam of the PNPI synchrocyclotron has a fixed energy of 1 GeV, a method of energy reduction by beam absorption in a copper degrader was applied in order to obtain proton beams with energies in the range from 200 to 900 MeV [1]. The proton energy was measured by the time-of-flight (TOF) method. The TOF spectra analysis showed that π^+ mesons were practically absent. The beam diameter at the target chamber location for all proton energies did not exceed 40 mm. The beam profile was measured by a thin scintillation counter, which scanned the beam in two orthogonal directions. The beam divergence was determined by monitoring the beam profile at the chamber inlet, outlet and in its centre at each proton energy variation. The beam intensity distribution on the target was a 2-dimensional normal distribution with the FWHM not larger than ~ 18 mm.

In the present experiment, the fission fragment detector comprised an assembly of two identical gas PPACs with the target to be studied between them. The PPACs provide a large solid angle for fragments registration, have a high efficiency for fragments detection, and have good time characteristics (better than 300 ps time resolution for fission fragments). The latter property, together with the PPAC insensitivity to neutrons, photons and light charged particles with minimal energy loss in the matter, makes PPACs extremely favorable tools for accelerator experiments, allowing one to place them in a direct proton beam.

PPAC pulse amplitudes were determined both by the specific energy losses of the detected particles in heptane and by the gas gain value. The latter depends on the voltage between the anode and cathode, so the detection efficiency could be controlled by setting a proper voltage. By appropriate choice of the voltage value, one can introduce a threshold selection criterion. Nevertheless, it is not sufficient to employ only the threshold selection criterion when using a PPAC directly in the proton beam. In fact, the amplitude spectrum of the detected particles contains, together with the pulses of fission fragments, a considerable contribution of low-amplitude background events. These events are caused by various proton-induced nuclear reactions in the matter along the beam line. Such a low-energy component is strongly suppressed by the coincidence criterion switched on. Moreover, an analysis of amplitude correlations of the coinciding fragments allowed us to exclude almost all background events. Thus, in our experiment we used three criteria to select binary

fission events: a threshold criterion, coincidences, and a criterion of the total kinetic energy of the detected coincident particles (the amplitude correlations).

A PPAC is so thin that it does not harm the beam characteristics when located in the beam. For this reason, several assemblies with various targets could be readily placed into the beam. This allowed us to reduce considerably the measurement time. In the real experiment, up to six assemblies were used at the same time. The layout of the set-up including the reaction chamber with the fission event detectors and the proton monitoring system is shown in Fig. 1. The main part of the set-up is a hermetic chamber with six detector assemblies, each assembly comprising two PPACs and a target in between.

Before entering the reaction chamber, the proton beam passed three scintillation counters (S1&S2&S3), combined *via* the coincidence scheme for direct proton counting. Just downstream of the reaction chamber, a polyethylene target $(CH_2)_n$ was placed. Protons elastically scattered from this target were detected by a two-arm scintillation telescope (S4&S5&S6), which served as a secondary beam monitor.

Direct counting of the incident protons with a scintillation counter telescope was used for beam monitoring. This method provides good monitoring accuracy only for low intensity beams, up to $\sim 10^5$ s^{-1}. However, for experiments with lead, thallium and gold nuclei, which have small fissility, one needs much higher beam intensity. For this reason, measurements were performed at two intensity values of the proton beam: $\sim 10^5$ s^{-1} and 10^6–10^7 s^{-1}. In the latter case, the beam monitoring was done by two methods: 1) by detecting fission events from a calibration target of ^{238}U residing in the reaction chamber, and 2) by detecting events of *pp* scattering on an auxiliary $(CH_2)_n$ target with the two-arm scintillation telescope (S4&S5&S6). Both methods were previously calibrated at low intensity ($< 2 \times 10^5$ s^{-1}) with the direct monitoring telescope (S1&S2&S3). A comparison of both methods at high intensity has shown agreement of the results within $\sim$ 3–6 % at all energies from 200 to 1000 MeV. The calibration procedure for secondary monitoring was described in detail in [2]. The target to be investigated was a thin layer of material deposited by vacuum evaporation on one of the electrodes of the PPAC assembly. The thickness of targets was determined by measuring the energy losses of α-particles passing through the target. So, using the methods of detection of the binary fission events and beam monitoring described in [2] we have measured the fission cross sections for each target at nine proton energies.
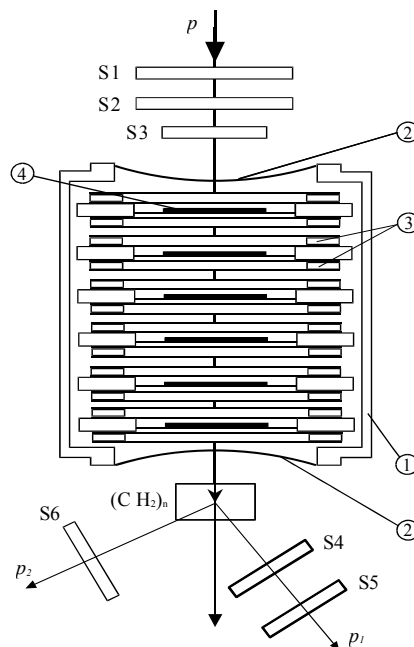

Fig. 1. Experimental set-up: 1 – chamber filled with heptane; 2 – entrance window; 3 – PPACs; 4 – target; S1–S6 – scintillation counters

The cross section calculation procedure comprised the following steps.

1. Background subtraction after analysis of the 2-dimensional amplitude distribution of the detected events. The number of background events amounted to 3−5 % of the total number of the detected events.

2. Determination of the solid angle for fission event detection for each assembly. The calculation was done by Monte Carlo simulations which took into account the proton beam profile on the target, the geometry of the fission fragments detection, the fragments mass and their energy distributions, as well as the anisotropy of the fragments angular distributions in the laboratory system due to the longitudinal momentum component of the fissile nucleus. The statistical accuracy of the solid angle calculations was about 0.1 %.

3. Estimation of the undetectable fraction of the fission events caused by the energy loss of fission fragments in the target, in its supporting foil, and in the PPAC electrodes. The undetectable part of the events depended on the target nucleus and thickness, and was about 4 %.

4. Determination of the integral proton flux through the target, with the account of the scintillation telescope efficiency and the probability of arrival of more than one proton in a microbunch at low intensity.

5. Determination of the normalization factors to calculate the proton flux at high intensity *via* the counting rate of the *pp*-scattering monitor and the fission counting rate from the calibration target.

The measured cross sections for fission of the [197]Au, [203]Tl, [206]Pb, [207]Pb, [208]Pb and [nat]Pb nuclei are shown in Table 1. For most of the nuclei, the presented data were averaged over the results of several measurements, the errors being determined mainly by the monitoring errors and the uncertainties in the target thickness.

Table 1

Proton induced fission cross sections (mb)

Energy, MeV	[197]Au	[203]Tl	[206]Pb	[207]Pb	[208]Pb	[nat]Pb
207	35 ± 2	63 ± 5	104 ± 6	80 ± 9	66 ± 6	60.5 ± 3.5
302	47 ± 2	81 ± 5	127 ± 6	100 ± 10	82 ± 6	84 ± 4.5
404	58 ± 28	104 ± 5	145 ± 6	134 ± 8	100 ± 6	110 ± 6
505	67 ± 2	123 ± 6	164 ± 6	135 ± 7	110 ± 7	118.5 ± 6
612	74 ± 3	116 ± 6	168 ± 6	136 ± 7	120 ± 7	127 ± 6.5
702	81 ± 3	147 ± 8	178 ± 7	143 ± 7	132 ± 8	132.5 ± 9.5
802	85 ± 4	144 ± 8	189 ± 8	144 ± 7	135 ± 8	131 ± 8.5
899	87 ± 4		182 ± 7	146 ± 7	130 ± 8	133.5 ± 7.5
1000	78 ± 5	126 ± 8	180 ± 7	144 ± 7	129 ± 8	129 ± 8.5

The energy dependences of the fission cross sections obtained in the present experiment for [197]Au and [203]Tl are shown in Figs. 2 and 3 together with the EXFOR data for the energy range 40 MeV $< E_p <$ 1 GeV. The closed circles represent the experimental results that were used to get the parameters of the approximation curve. The open circles represent the data that were rejected due to their large deviations from the average values. For the first approximation, an exponential function was used:

$$\sigma_f = \sigma_1 - C_1 \exp(-E_p / t_1), \qquad (1)$$

where σ_1 is the asymptotic value of the fission cross section, C_1 and t_1 are free parameters. The parameter values obtained by the fit are presented in Table 2. The values of χ^2 / ν, where ν is the number of degrees of freedom, are listed in the last column of Table 2. They confirm the reliability of our approximations.

There were no experimental data on cross sections for fission of lead isotopes by protons in the energy range 200–1000 MeV. We have performed measurements to obtain information on the energy dependence of the isotopic effect in this energy range. The isotopic effect consists in the dependence of the total fission cross sections on the fissility parameter (Z^2 / A) of the target nucleus, where Z is its charge number and A is its mass number. As is well known, this parameter reflects the ratio of the Coulomb energy of a charged liquid drop to its surface tension energy. The electric charge tends to break the drop, while the surface tension maintains its integrity. The isotopic effect is relatively weak, but the existing fission models underestimate it even more. Its experimental study is therefore of interest for physics of nuclear fission.
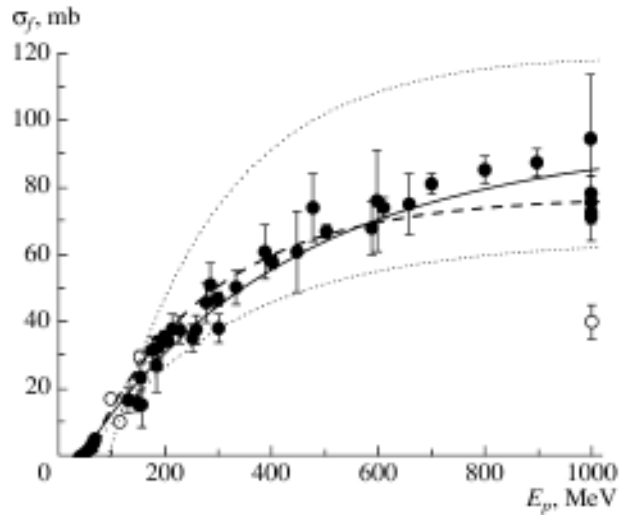
Fig. 2. Energy dependence of the proton induced fission cross sections for ^{197}Au. The closed circles stand for the experimental results used here to derive the approximation by Eq. (1) (solid curve); the open circles are the ignored data. The dashed curve is the approximation from [3], while the lower and upper dotted curves represent the results of model calculations from [4] and [5], respectively
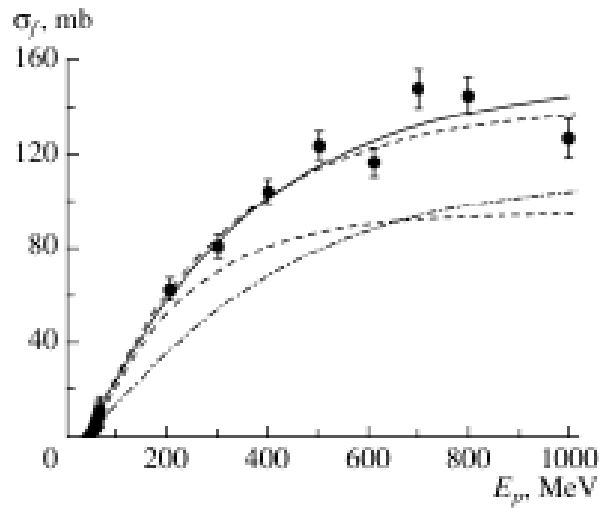

Fig. 3. Energy dependence of the proton induced fission cross sections for ^{203}Tl. The displayed points are the experimental data measured in our experiment and in experiment [6] in the energy region of $E \sim 30$ MeV, and used here for the approximation by Eq. (1) (solid curve). The upper and lower dashed curves represent, respectively, our approximations for ^{208}Pb [7] and Prokofiev's approximation for ^{205}Tl [3]. The dash-dotted curve is our prediction for the energy dependence of the cross section for proton induced fission of ^{205}Tl

Table 2

Parameters for the Eq. (1) approximation for different nuclei

Parameters	σ_1, mb	C_1, mb	t_1, MeV	χ^2 / ν
^{197}Au	93 ± 2	103 ± 2	396 ± 17	0.99
^{203}Tl	152 ± 8	172 ± 6	329 ± 35	0.99
^{206}Pb	179 ± 4	225 ± 5	181 ± 12	0.99
^{207}Pb	144 ± 3	186 ± 5	168 ± 11	0.99
^{208}Pb	140 ± 4	163 ± 4	278 ± 13	0.97

252

We have studied this effect for fission of uranium isotopes by protons with energies $E_p = 200–1000$ MeV. It has been found that it runs from ~ 30 mb for the difference between ^{235}U and ^{238}U fission cross sections per each missing neutron up to ~ 80 mb for half of the difference between the ^{233}U and ^{235}U fission cross sections. The relative contribution from the isotopic effect in uranium (3 ± 1 %) is almost independent of the proton beam energy [8].

The measurement results contained in the EXFOR database [3] show that the increase in total fission cross sections for lead isotopes at $E_p \approx 50$ MeV is ~ 40 % per each missing neutron. For platinum nuclei, the relative contribution from the isotopic effect is even larger [6]. Its absolute contribution increases with the fissility parameter (Z^2/A).

There were no experimental data on cross sections for fission of lead isotopes by protons in the energy range 200–1000 MeV. We have performed such measurements to obtain information on the energy dependence of the isotopic effect in this energy range.
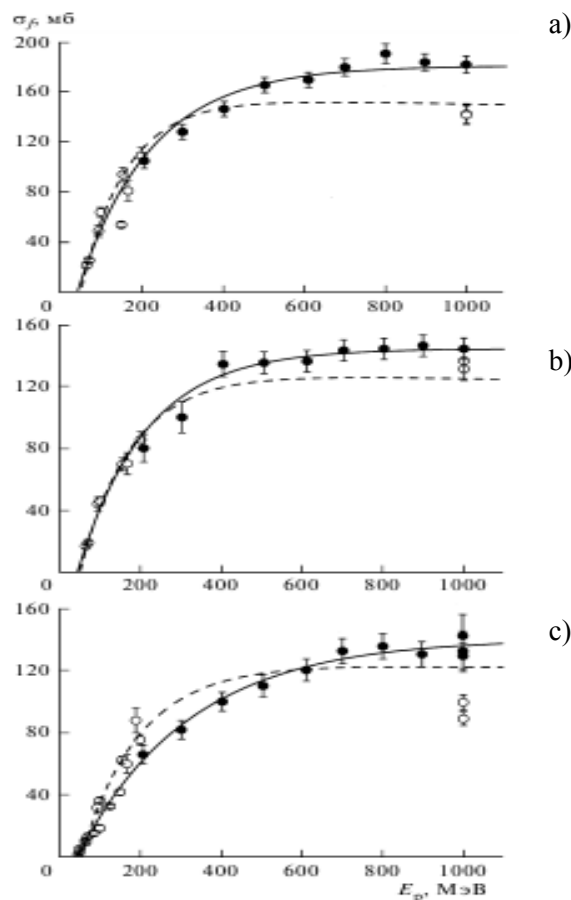

Fig. 4. Energy dependences of the total cross sections for fission of: a – ^{206}Pb; b – ^{207}Pb, and c – ^{208}Pb nuclei by protons. Closed circles are the results of our measurements, open circles are the EXFOR database values [3]. Solid and dashed curves are our approximations and approximations by A.V. Prokofiev [3]

In Table 1, the measured total cross sections for fission of lead isotopes are presented. They are also shown in Fig. 4a–c by closed circles, together with the cross sections for fission by 1 GeV protons that we had published previously [9]. The EXFOR database values [3] are represented by open circles. The absence of error bars means that the authors considered the experimental errors to be equal to 10 % of the corresponding total fission cross section. The data were approximated by the exponential function.

The absolute increase in the total cross sections for fission of ^{208}Pb and ^{238}U nuclei by protons with energies of 200–1000 MeV after a loss of a neutron was almost identical, *i.e.*, 20–30 mb, despite these cross sections are different by more than a factor of 10. As is well known, a decrease in the parameter (Z^2/A) is

accompanied by an increase of the fission barrier of heavy nuclei. The higher the fission barrier, the larger the relative contribution of the isotopic effect should be.

The measured total cross sections for fission of uranium and lead isotopes induced by protons indicate a progressive increase of the isotopic effect as the nucleus mass decreases, approximately in proportion to its fissility parameter (Z^2/A).

References

1. N.K. Abrossimov, V.G. Vovchenko, V.A. Eliseev, E.M. Ivanov, Yu.T. Mironov, G.A. Riabov, M.G. Tverskoy and Yu.A. Chestnov, Preprint PNPI-**2525**, Gatchina (2003).
2. V.G. Vovchenko, L.A. Vaishnene, Yu.A. Gavrikov, A.A. Kotov, V.I. Murzin, V.V. Poliakov, S.I. Trush, O.Ya. Fedorov, Yu.A. Chestnov, A.V. Shvedchikov and A.I. Shchetkovski, Preprint PNPI-**2532**, Gatchina (2003).
3. A.V. Prokofiev, Nucl. Instr. Meth. Phys. Res. A **463**, 557 (2001).
4. V.S. Barashenkov, F.G. Gereghi, A.S. Iljinov *et al.*, Nucl. Phys. A **222**, 204 (1974).
5. M.H. Simbel, Z. Phys. A **333**, 177 (1989).
6. O.A. Zhukova, A.V. Ignatyuk, M.G. Itkis *et al.*, Yad. Fiz. **26**, 473 (1977).
7. L.A. Vaishnene, V.G. Vovchenko, Yu.A. Gavrikov *et al.*, Izv. Akad. Nauk, Ser. Fiz. **74**, 529 (2010).
8. A.A. Kotov, L.A. Vaishnene, V.G. Vovchenko *et al.*, Izv. Akad. Nauk, Ser. Fiz. **71**, 837 (2007) [Bull. Russian Acad. Sci. (English Transl.) **71**, 809 (2007)].
9. L.A. Vaishnene, L.N. Andronenko, G.G. Kovshevny *et al.*, Z. Phys. A **302**, 143 (1981).